Benchmarking Standing Stability for Bipedal Robots

Juan A. Castano, Eugenio Manuel Espuela, Jaime Ramos Rojas, Enrico Mingo Hoffman, Chengxu Zhou

IEEE Access
Multidisciplinary | Rapid Review | Open Access Journal

Date of publication xxxx 00, 0000, date of current version xxxx 00, 0000.

Digital Object Identifier

Benchmarking Standing Stability for Bipedal Robots

JUAN A. CASTANO[1], EUGENIO MANUEL ESPUELA[1], JAIME RAMOS ROJAS[1,2], ENRICO MINGO HOFFMAN[3], and CHENGXU ZHOU[4]

[1]Department of Applied Mathematics, Science and Material Engineering, and Electronics Technologies, School of Experimental Sciences and Technology, Campus de Mostoles, Rey Juan Carlos University, 28933 Madrid, Spain, https://ror.org/01v5cv687
[2]International Doctoral School of Rey Juan Carlos University, 28933 Madrid, Spain
[3]Université de Lorraine, CNRS, Inria, LORIA, 615 Rue du Jardin-Botanique, Villers-lès-Nancy, France
[4]Department of Computer Science, University College London, UK.

Corresponding author: Juan A. Castano (juan.castano@urjc.es), Chengxu Zhou (chengxu.zhou@ucl.ac.uk).

This work was supported by the Royal Society [grant number RG\R2\232409], Grant PID2021-123657OB-C32 funded by MCIN\AEI\10.13039\501100011033, by "ERDF A way of making Europe", and by the French National Research Agency (ANR) under the project ANR-24-CE33-0753-01 (MeRLin).

ABSTRACT Developing robust benchmarking methods is crucial for evaluating the standing stability of bipedal systems, including humanoid robots and exoskeletons. This paper presents a standardized benchmarking procedure based on the Linear Inverted Pendulum Model and the Capture Point concept to normalize the maximum angular momentum before falling. Normalizing these variables establishes absolute and relative benchmarks achieving comprehensive comparisons across different bipedal systems. Simulations were conducted on two humanoid robots, COMAN and WALK-MAN, to validate the approach, demonstrating its applicability to robots of various sizes and configurations. Furthermore, the same benchmarking method was applied to the therapeutic exoskeleton H3, illustrating its potential to optimize mechanical design and therapeutic performance. The results indicate that this standardized procedure provides a valuable tool for assessing and improving the stability of anthropomorphic robotic systems, providing insights into both hardware capabilities and control strategies.

INDEX TERMS Benchmark, Standing Stability, Humanoid Robots, Exoskeletons

I. INTRODUCTION

A. SYNOPSIS

Over the past decade, the issue of benchmarking the standing stability of bipedal systems, such as humanoid robots and exoskeletons, has become more prominent due to a growing understanding of the importance of positively influencing mechanical design considerations [1]. Benchmarking is a critical component in identifying the functional characteristics of a robot after evaluating its inherent mechanical performance for a specific task. The systematic standardization of metrics and approaches developed through effective benchmarking allows developers to focus on best practices, eliminating the need to create substandard solutions to obscure problems caused by overlooked biomechanical design considerations [2].

Bipedal robots derive their name from their distinctive anthropomorphic characteristics, making it clear that the primary goal of building these systems is to replicate a biological solution. Thus, a method to synthesize a true benchmark from bipeds to humans is quintessential; it will not only provide an excellent indication of physical performance capabilities but also present an incentive to achieve optimal compliant behavior [3]. Ho Hoang *et al.* [4] demonstrated critical benchmarking criteria when deriving quantities for bipedal stability. Observe that stable bipedal walking is derived from the balancing of angular momentum generated by the various oscillating limbs; this indicates the same for standing stability due to the use of the same biological quantities of motion [5].

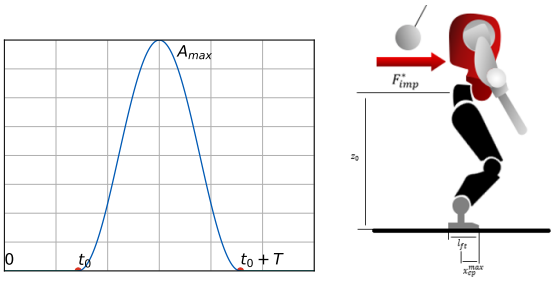

(a) Impulsive disturbance (b) Standing stability test

FIGURE 1: The proposed benchmarking test setup.

Benchmarking bipedal robots' stability and comparing different designs has proved to be challenging despite their human likeness [6]. This difficulty arises because designers have differentiating metrics that include weight, height, joint length, COM position, ifnextchar.etcetc., in which designers do not have a standardized specification to consider during production [2]. This means that developers have various approaches when building humanoid or exoskeleton robots based on their engineering intuition and experience over systematic practice. Subsequently, there is currently no single regulatory and standardized standing stability benchmarking method; despite engineers developing robots acquiring exceptional static and dynamic stabilization characteristics. This problem is also present when designing exoskeletons for therapy or as augmentation systems [7]. The performance of such systems when performing either balancing or other tasks is evaluated considering human capacity and does not provide a guide to the mechanical design by itself. In this sense, applying various benchmarking criteria can help identify the best practices in the literature by enabling appropriate comparisons. More specifically, when evaluating therapeutic performance, as in [8], having metrics such as the one proposed in this paper, might provide a clearer idea regarding the effectiveness of the proposed therapy and used device.

B. RELATED WORK

The application of bipedal locomotion is undoubtedly inspired by human movement. Humans have unprecedented standing stability, and thus human stability analysis is essential. However, the high non-linearity of human movement and joint actuation makes this analysis difficult. Ho Hoang *et al.* [4] developed a benchmarking scheme for bipedal locomotion based on angular momentum. Another human stability/gait analysis issue is comparing measurements to a single subject. Hof [9] developed a table that presents dimensionless mechanical quantities concerning human gait analysis - shown in Table I. The table's practicality lies in its simplicity, yet it is highly effective for comparing various subjects. This paper leverages the table by incorporating quantities like angular momentum to normalize the data.

To understand the requirements of the most intuitive benchmark for standing stability, particular tasks must be identified from a common taxonomy [9]. Concerning static and locomotion, Fleishman *et al.* [10] identified various sensorimotor abilities which affect these skills. The classification of the required bipedal motor skills is derived from the tasks and the environment in which a humanoid operates. Hof *et al.* [5] reduced many of the unnecessary motor abilities and developed a subset focused on lower limb performance, which we utilize in this work. The same paper also identifies various benchmarks categorized by performance and human likeness, both covered in segments of this paper. Toricelli *et al.* [2] further developed these ideas by stating various criteria that can assess human-like robotic behavior such as measuring the Center of Mass (CoM) displacement driven by manual perturbations.

TABLE I: Normalization of kinematic and dynamic variables, adopted from [9]. m_0 overall mass, l_{leg} leg length, g gravitational acceleration, z_0 overall CoM height. Symbols with "^" are dimensionless benchmarked quantities.

Quantity	Symbol	Dimension	Normalization by l_0 ($l_0 = l_{leg}$ or z_0)
Mass	m	M	$\hat{m} = \frac{m}{m_0}$
Time	t	T	$\hat{t} = \frac{t}{\sqrt{l_0/g}}$
Frequency	f	T^{-1}	$\hat{f} = \frac{f}{\sqrt{g/l_0}}$
Length	l	S	$\hat{l} = \frac{l}{l_0}$
Velocity	v	ST^{-1}	$\hat{v} = \frac{v}{\sqrt{gl_0}}$
Acceleration	a	ST^{-2}	$\hat{a} = \frac{a}{g}$
Linear Momentum	p	MST^{-1}	$\hat{p} = \frac{p}{m_0\sqrt{gl_0}}$
Force	F	MST^{-2}	$\hat{F} = \frac{F}{m_0 g}$
Torque	τ	$\mathrm{MS}^2\mathrm{T}^{-2}$	$\hat{\tau} = \frac{\tau}{m_0 g l_0}$
Inertial	I	MS^2	$\hat{I} = \frac{I}{m_0 l_0^2}$
Angle	θ	(already dimensionless)	
Angular Velocity	ω	T^{-1}	$\hat{\omega} = \frac{\omega}{\sqrt{g/l_0}}$
Angular Acceleration	$\dot{\omega}$	T^{-2}	$\hat{\dot{\omega}} = \frac{\dot{\omega}}{g/l_0}$
Angular Momentum	L	$\mathrm{MS}^2\mathrm{T}^{-1}$	$\hat{L} = \frac{L}{m_0 l_0\sqrt{gl_0}}$
Energy	E	$\mathrm{MS}^2\mathrm{T}^{-2}$	$\hat{E} = \frac{E}{m_0 g l_0}$
Power	P	$\mathrm{MS}^2\mathrm{T}^{-3}$	$\hat{P} = \frac{P}{m_0 g\sqrt{gl_0}}$

A qualitative approach, which comprises the robots' actual structural parameters, for robotic benchmark is inherently difficult. Many arguments have been proposed for the use of alternative approaches. For example, various researchers proposed using competitions to analyze specific task performance [11]. Stasse *et al.* [12] considered a task-based high-level approach and tried to make the benchmark values more significant using a statistical performance analysis. There have been many propositions for objective-based performance benchmarking. However, these approaches are impartial and do not articulate specific analytical design considerations for the support of a better design. High-level task-based methods are intuitive but unfortunately do not provide a low-level biomechanical analysis, which an engineer can exploit to gain a more detailed understanding of the robot's potential capabilities.

Due to the ability to intuitively analyze the subjects' metrics and generate dynamics models, abstract modeling of a biped leg and its support is one of the most conventional methods in the mathematical modeling of humanoid robots. A notable model that we use to evaluate our systems in this paper is known as the Linear Inverted Pendulum Model (LIPM) [13], which is widely used for legged locomotion [13], [14]. The LIPM provides the ability to understand specific foot placement strategies, without modeling the foot itself [15]. The ad-

vantages of the LIPM derive from the simplicity and linearity of the model, and how the movement of the CoM can be determined from a simple-form linear differential equation [16].

The Capture Point (CP) [17] is a concept used to compute the required stepping location for a robot or human to remain stable - based on a LIPM; thus now being one of the fundamental criteria for bipedal walking and stability control [18]. If the CP lies outside of the support polygon, the LIPM-controlled robot will result in falling. Dynamic actions such as stepping can be taken to enlarge the support polygon and prevent falling. In this paper, we leverage the Capture Point (CP) concept to develop a benchmarking scheme for standing stability, given the practicality of this approach.

As studied in [7], these concepts have been used in various exoskeleton technologies; however, a specific bench to compare them has not been presented yet. In this regard, different approaches have been released that analyze the performance of the equipment from a practical point of view. In [19] for example, the authors evaluated the performance of a low-limb exoskeleton for ankle augmentation during a balance task. The authors assess different metrics related to stepping modification due to the use of the exoskeleton. Performance is compared across different participants and overall results are analyzed; however, no specific metrics are given, and results cannot be easily extrapolated to similar technologies since the tasks performed are subject-dependent and no normalization is given. A similar study is considered in [20] where a passive leg support system is evaluated during slippery conditions evaluating the fall probability while wearing such a system over 6 participants. Once again, no standardization is given, and the protocols are subject-dependent. In [21], [22] a back support exoskeleton's performance is evaluated during balancing and fall recovery. Once again, several trials with different subjects are studied and gait metrics are compared. However, these metrics will not provide comparison tools against similar hardware.

The previous works are focused on augmentation exoskeletons; however, when referring to therapeutic exoskeletons as in [23], the performance metrics are given on the patient impact [8]. In this case, the authors present results over different training regimens with different subjects and exoskeletons. Although progress comparisons can be made, patient dependence and therapeutic variability make it difficult to compare hardware performance. In this regard, the present benchmarking aims to provide a standardization tool when analyzing the mechanical performance of the exoskeleton from the balance point of view. Even though it has not been tested with subjects in this work, validation of the methodology with different hardware is provided, showing positive results for future studies.

From the specific perspective of balancing, as reported in [24], the use of exoskeletons in working environments affects the response capability of workers against different scenarios. In that paper, the authors evaluate workers falling risk while performing carpentry-related tasks. The effects that wearing and exoskeleton have are also studied in [25] where the authors analyze the impact of wearing industrial exoskeletons over different manufacturing phases and analyze their potentiality as well as the negative effects that might be introduced. As discussed by the authors by wearing these elements, certain manufacturing phases might be improved, however, awareness of new sources of musculoskeletal disorders and accidents should be addressed considering the user familiarization with the hardware since long use periods might lead to new musculoskeletal disorders while occasionally use is more likely to produce accidents due to the cognitive load on the exoskeleton usage that can affect negatively the motor control performance including balancing [26]. The falling risk is analyzed when wearing an active back-support exoskeleton by studying the foot behaviors under different conditions, however, balancing under external disturbances itself is not reported, though should be considered as a fundamental capability in both therapeutic and occupational exoskeletons. This is reflected in [27], where several exoskeletons are benchmarked under different task scenarios including dynamics and isometric ones. In that work, no metrics are provided and balancing capabilities are not considered. On this matter, [28] developed the *"Benchbalance"* which is a push device that allows recording the disturbance data to facilitate the repeatability when disturbing a subject wearing or not exoskeletons. Results show the applied impulses at different body parts and the subjects' reactions to them. However, no metrics on the static balancing are given.

C. CONTRIBUTION

This work presents an ideal approach to a standardized benchmarking procedure regarding the maximum standing stability of any bipedal robot, which can be simplified by a LIPM, through the absolute and relative normalization of the inherent angular momentum required to initiate the falling of a robot. The proposed benchmark aims to institutionalize the level of standing stability that a bipedal robot inherits from its nominal design characteristics. Given the robot's elementary structural parameters, the primary focus is on bipedal robots of any size. The robots are subject to examinations from two perspectives to ensure full practicality and rationality of the benchmark evaluation. First, the robots are benchmarked against absolute human data to generate a quantitative understanding of how they perform relative to ourselves; and second, their relative normalized LIPM data so the performance can be quantified against themselves. In addition, the benchmark can test software components, such as balancing algorithms and how they perform against their respective models. The benchmark presented is also applied to a real exoskeleton, demonstrating its generality and applicability beyond bipedal humanoid robots.

We first describe the relative human parameters in Section II, in which the normalization procedures for benchmarking are also given. The simulated and analytical results of two humanoid bipedal robots with distinctive dimensions are presented with various controllers and structural parameters respectively in Section III. Later, in Section IV, the proposed

benchmark is applied to the H3 therapeutic exoskeleton, both in simulation and real hardware. The precedence, value, and limitations of the benchmarking procedure are discussed in Section V and conclusions are given in Section VI.

II. ANALYTICAL BENCHMARKING PROCEDURE

In this section, we design the bipedal standing stability benchmark test and identify the required implementation criteria. To do so, this work considers that humanoid robots and exoskeletons have very similar bio-mechanical structures to humans but very diverse full-body metrics. Therefore, we can intuitively use human parameters as a means of absolute comparison. This implies that using humans as a benchmark will hold very pragmatic and real stability characteristics, providing a performance index in a self-relational quantity. For this purpose, we need to define the nominal values relative to the LIPM. For our nominal human normalization data presented in Section III, Table II, the mass, CoM height, and foot length must be defined. The average mass and foot length of a human is estimated to be 60.2 kg and 0.26 m, respectively [29]. We assume that the adult's average CoM height is 1.0 m, approximately 10% of the average leg length [30] over the hip. With these parameters, data analysis can be performed based on a normalized set of parameters that allow proper comparisons.

The test is designed based on an impulsive disturbance applied to the subject's CoM in the sagittal plane, as shown in Fig. 1(b). By applying an external impulsive disturbance, we can accurately determine the angular momentum and effectively impart velocity to the CoM, enabling us to develop our CP and LIPM-based approach. We exploit the CP and LIPM to derive normalization of various kinematic and dynamic parameters based on Table I. To intuitively analyze the standing stability, we use a capture ratio, α (detailed in Section II-C), which complements the normalization process with the consideration of biped's foot size.

A. IMPULSIVE DISTURBANCE

We define the disturbance as an impulsive force $F_{\text{imp}}(t)$ acting on a standing robot during a period t_{imp}, which generates an impulsive torque $\tau_{\text{imp}}(t)$ about the feet, resulting in a change of angular momentum.

The impulsive force (in both continuous and discrete forms) applied at the CoM will impart linear momentum given by:

$$p_{imp} = \int_0^{t_{imp}} F_{imp}(t)dt = \frac{\sum_0^k F_{imp}(k)}{t_{imp}}. \tag{1}$$

Thus, the corresponding angular momentum at the CoM *w.r.t* foot, L_{imp}, is:

$$L_{imp} = p_{imp} z_0, \tag{2}$$

where z_0 is the CoM height.

Assuming a half-sinusoidal profile for the impulsive disturbance, as illustrated in Fig. 1(a), with a maximum amplitude A_{imp} and period t_{imp}, the linear momentum can be calculated by integrating over time using (1):

$$p_{imp} = \int_0^{t_{imp}} A_{imp} \sin(\frac{\pi t}{t_{imp}})dt = \frac{2A_{imp}t_{imp}}{\pi}. \tag{3}$$

B. LIPM DYNAMICS

A standing humanoid robot's CoM dynamics can be simplified as a LIPM [13], which consists of a point CoM and a massless telescopic leg. The dynamics of the LIPM describe the movement of the CoM by

$$\ddot{x} = \frac{g}{z_0}x, \tag{4}$$

where x is the CoM position in the local frame at the supporting foot according to the axial direction.

Solving (4) for x leads to:

$$x(t) = x_0 \cosh(\frac{t}{T_c}) + T_c\dot{x}_0 \sinh(\frac{t}{T_c}), \tag{5}$$

$$\dot{x}(t) = \frac{x_0}{T_c} \sinh(\frac{t}{T_c}) + \dot{x}_0 \cosh(\frac{t}{T_c}), \tag{6}$$

where $T_c = \sqrt{z_0/g}$ is the time constant of a LIPM and x_0 and $\dot{x}_0$ is the initial position and velocity respectively.

C. DISTURBANCE NORMALIZATION

To analyze the occurrence of instability, we define the maximum CP location. We use the maximum displacement limit which the CP has to emulate to remain stable, after the directional movement of the CoM at the instantaneous state just before falling [18], [31]. The CP, x_{cp}, is defined by

$$x_{\text{cp}} = x + \sqrt{\frac{z_0}{g}}\dot{x} = x + T_c\dot{x}. \tag{7}$$

Falling will happen when the CP goes outside of the support polygon; therefore, considering the sagittal plane, the maximum distance that the CP could travel without losing balance is formulated as

$$x_{\text{cp}}^{\max} = l_{\text{ft}} - x_0, \tag{8}$$

where l_{ft} is the foot length, x_0 is the initial CoM position. Considering the maximum CP among the static model, instability occurs when the following is satisfied:

$$x + \sqrt{\frac{z_0}{g}}\dot{x} > x_{\text{cp}}^{\max}, \tag{9}$$

which will result in falling, due to the CP exceeding the support polygon. Using CP and LIPM makes it difficult to derive the position and velocity directly from the disturbance input. However, designing the test this way is the most effective approach due to the experimental constraints. As shown from the denominators in Table I, one unit of change in velocity causes one unit change in momentum in reverse. Therefore, in the standing test, a nominal disturbance is defined and applied to the humanoid, resulting in a proportional change in the robot's normalized velocity. After a certain time t_{cp}, the location of the CP will relocate to a region of instability.

Therefore, we must derive the CP dependent on t_{cp}, thus substituting (5) and (6), into (7) we obtain the following:

$$x_{\text{cp}}(t_{\text{cp}}) = (x_0 + T_c\dot{x}_0)(\cosh(\frac{t_{\text{cp}}}{T_c}) + \sinh(\frac{t_{\text{cp}}}{T_c})). \tag{10}$$

For the standing test, $x_0 = 0$ because the robot is initially stationary, therefore, (10) becomes:

$$e^{\frac{t_{cp}}{T_c}} = \frac{x_{\text{cp}}(t_{\text{cp}})}{T_c\dot{x}_0}. \tag{11}$$

Solving for t_{cp}, (11) becomes:

$$t_{cp} = T_c \ln\left(\frac{x_{\text{cp}}(t_{cp})}{T_c\dot{x}_0}\right). \tag{12}$$

Respective of a defined length, l_0 we can define a new equation for $x_{\text{cp}}^{\max}$:

$$x_{\text{cp}}^{\max} = \alpha l_0. \tag{13}$$

where, α is the *capture ratio*. The capture ratio is defined by the maximum CP location within a stable region, relative to the distance of measurement, l_0. l_0 is a length measurement generalization and could substituted for leg length or CoM height. We use the CoM height z_0 for the normalization in this paper.

Therefore, substituting (13) into (12), the maximum initial CoM velocity $\dot{x}_0^{\max}$ that will not cause falling can be obtained at when $t_{\text{cp}} = 0$, so that

$$\dot{x}_0^{\max} = \frac{x_{\text{cp}}^{\max}}{T_c} = \frac{\alpha l_0}{T_c} = \alpha l_0\sqrt{\frac{g}{z_0}}. \tag{14}$$

Normalizing (14) by substituting the CoM height, z_0, for l_0, then $\dot{x}_0^{\max} = \alpha\sqrt{z_0 g}$, thus, according to Table I, the normalized velocity can be calculated as:

$$\hat{x}_0^{\max} = \frac{\dot{x}_0^{\max}}{\sqrt{z_0 g}} = \alpha, \tag{15}$$

where the quantity $\hat{x}_0^{\max}$ is the normalized value. Therefore, if we use the caption ratio α with the normalization denominators in Table I, a new set can be defined by

$$\begin{cases} D_{p_{imp}} = \alpha m_0\sqrt{gz_0}, \\ D_{L_{imp}} = \alpha m_0 z_0\sqrt{gz_0}, \\ D_{F_{imp}} = \alpha m_0 g, \\ D_{\tau_{imp}} = \alpha z_0 m_0 g, \end{cases} \tag{16}$$

where m_0 is the robot total mass, g is the gravitational constant, D_v is the LIPM based normalization quantity denominator of the variable v. Thus, the normalized angular momentum we use for our benchmark is determined by

$$\hat{L}_{\text{imp}} = \frac{L_{\text{imp}}}{D_{L_{\text{imp}}}} = \frac{L_{\text{imp}}}{\alpha m_0 z_0\sqrt{gz_0}}, \tag{17}$$

where L_{imp} is the impact angular momentum at CoM *w.r.t* foot. The same can be completed for the human model where the respective variables are denoted as $\hat{L}_{\text{imp}}^H$, L_{imp}^H and $D_{L_{\text{imp}}}^H$.

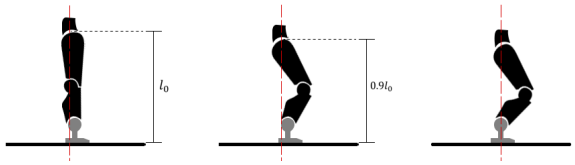

FIGURE 2: Three steps for benchmarking tests initialization. (a) the initial resting position, (b) the legs are bent to 90% of the total leg length and (c) moving pelvis to align the CoM at the center of the support polygon.

III. SIMULATIONS ON HUMANOID ROBOTS

In this paper, we compare COMAN [32], a child-size humanoid robot, and WALK-MAN [33], an adult-size humanoid robot, to benchmark their standing stability performance. The nominal quantities of normalization of angular momentum of each robot are determined, using the CP and LIPM-based approach in Section II A sagittal push-based simulation is conducted, illustrated in Fig. 1(b). An incremental impulsive disturbance is applied to the rear of the robot pelvis until falling occurs. Subsequently, the impact angular momentum is determined from the required tipping force. Successively, the robots' angular momentums are normalized by the humans and their respective nominal normalization quantity.

A. SIMULATION SETUP

To conduct the simulation itself, impulsive forces with a fixed duration

$$\text{t}_{imp} = \text{T}_c/2, \tag{18}$$

and an incremental amplitude F_{imp} are applied to the pelvis of the robot along the sagittal plane, that is, the positive axis x. According to the location of the application of the external perturbation, the equivalent force at the CoM is computed as:

$$\tau_f = F_{\text{imp}}^* l_{\text{imp}}^* = F_{\text{imp}} z_0, \tag{19}$$

where F_{imp}^* and l_{imp}^* are the impulsive force and location, respectively. F_{imp} is the equivalent force at the CoM.

Fig. 2 demonstrates how we set up the simulation. Fig. 2(b) shows how the initial kinematic state was modified by bending the knees by a factor of 0.9 of the total leg length to avoid singularities for balancing controllers. Fig. 2(c) demonstrates the final step, where the pelvis is moved to ensure that the CoM is aligned with the center of the foot, so that $x_{\text{cp}}^{max} = \frac{1}{2}l_{ft}$. Thus the capture ratio α can be calculated using (13). This regulates the approach so that results remain consistent and reproducible.

B. RESULTS

First, a total of nine simulations were carried out on the two humanoid robots to evaluate the effectiveness of the proposed benchmarking approach. Both robot models were modified by half-reducing the length of the feet accordingly. In addition, three balancing controllers were used in the COMAN simulations:

TABLE II: Standing stability benchmarking tests data of COMAN (C), WALK-MAN (W), and Exo-H3 (H3).

Quantity	Symbol	Human	C_1	C_2	C_3	C_4	C_5	C_6	W_1	W_2	W_3	$H3_1$	$H3_2$	$H3_3$	$H3_4$	$H3_5$	$H3_6$	$H3_7$	$H3_8$
Mass - kg	m_0	60.2	30.9	←	←	←	←	←	123.4	←	←	15.4	←	←	←	←	←	←	←
CoM height - m	z_0	1	0.492	←	←	←	←	←	0.952	←	←	0.567	←	←	←	←	←	←	←
max. CP traveling distance (8)	αz_0	0.15	0.1	←	←	←	0.05	0.2	0.16	0.08	0.32	0.15	0.077	0.08	0.085	0.09	0.085	0.077	0.15
max. CP traveling ratio (13)	α	0.15	0.203	←	←	←	0.102	0.407	0.168	0.084	0.336	0.264	0.136	0.141	0.15	0.159	0.15	0.136	0.264
Time constant - s	T_c	0.319	0.224	←	←	←	←	←	0.312	←	←	0.24	←	←	←	←	←	←	←
Nominal ang. mom. (16)	$D_{L_{imp}}$	24.80	6.79	←	←	←	3.40	13.6	60.3	30.2	120.7	5.4	2.8	2.9	3.1	3.2	3.0	2.8	5.4
Impact height - m	l^*_{imp}		0.498	←	←	←	←	←	1.0712	←	←	0.787	←	←	←	←	←	←	←
Foot length - m	l_{ft}		0.2	←	←	←	0.1	0.4	0.32	0.16	0.64	0.3	0.227	0.23	0.235	0.24	0.235	0.227	0.3
Impact duration - s	t_{imp}		0.112	←	←	←	←	←	0.156	←	←	0.193	0.2	←	←	←	0.12	0.12	0.2
Impact force amp. - N	F^*_{imp}		256.3	246.5	273.8	308.1	124.2	529.9	741.5	351.8	1536.8	37.6	37.6	38.72	41.59	44.28	62.66	55.95	69,220
Equi. force at CoM (19)	F_{imp}		259.4	249.5	277.2	311.8	125.7	536.4	834.3	395.9	1729.2	52.12	52.12	53.06	57.65	61.38	86.87	77.57	95,961
Impact lin. mom. at CoM (3)	p_{imp}		18.5	17.8	19.8	22.2	8.96	38.2	82.7	37.4	163.3	6.4	6.6	6.7	7.3	7.8	6.6	5.9	12.2
Impact ang. mom. at CoM to foot (2)	L_{imp}		9.1	8.7	9.7	10.9	4.4	18.8	78.7	35.6	155.4	3.63	3.76	3.83	4.16	4.43	3.76	3.36	6,933
Normalized ang. mom. to LIPM (17)	$\hat{L}_{imp}$		**1.34**	**1.29**	**1.43**	**1.61**	**1.30**	**1.38**	**1.30**	**1.24**	**1.35**	**0.68**	**1.34**	**1.32**	**1.35**	**1.36**	**1.22**	**1.203**	**1.207**
Normalized ang. mom. to Human	$\hat{L}^H_{imp}$	**1.0**	**0.32**	**0.31**	**0.34**	**0.39**	**0.16**	**0.66**	**2.78**	**1.32**	**5.77**	**0.15**	**0.15**	**0.16**	**0.17**	**0.18**	**0.15**	**0.13**	**0.28**

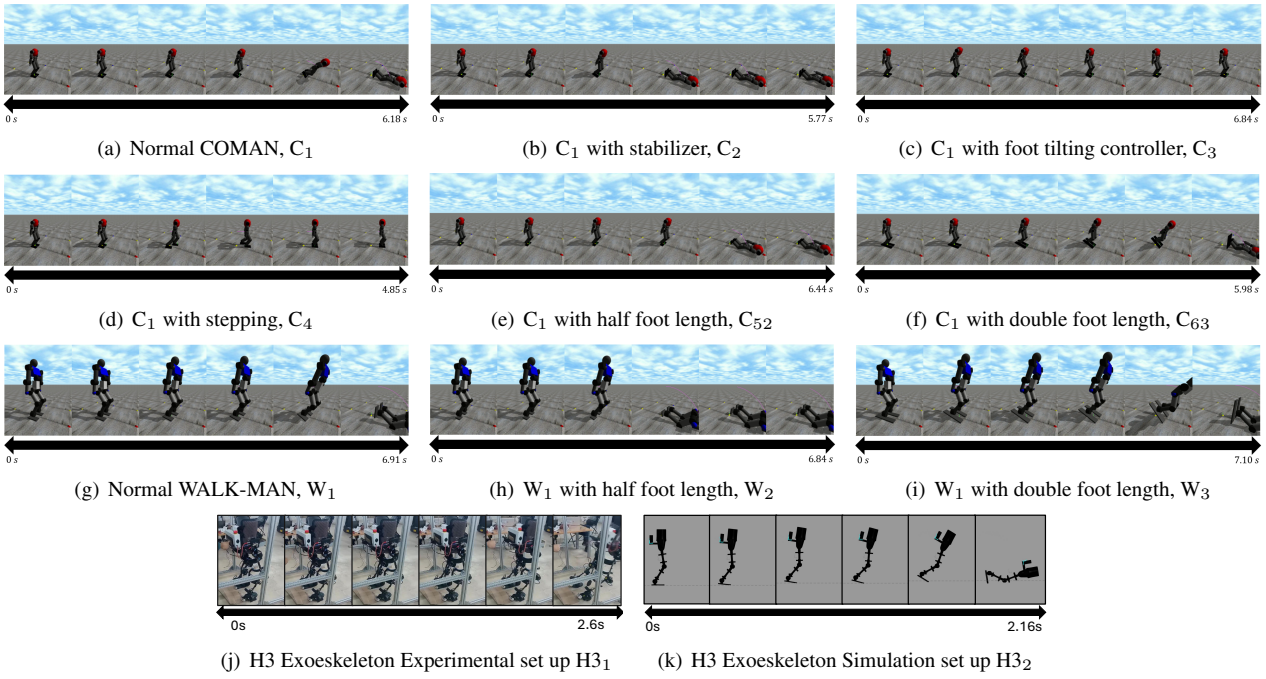

(a) Normal COMAN, C_1 (b) C_1 with stabilizer, C_2 (c) C_1 with foot tilting controller, C_3

(d) C_1 with stepping, C_4 (e) C_1 with half foot length, C_{52} (f) C_1 with double foot length, C_{63}

(g) Normal WALK-MAN, W_1 (h) W_1 with half foot length, W_2 (i) W_1 with double foot length, W_3

(j) H3 Exoeskeleton Experimental set up $H3_1$ (k) H3 Exoeskeleton Simulation set up $H3_2$

FIGURE 3: Snapshots showing the incrementally applied disturbance to determine maximum impact force, F_{imp}.

- a stabilizer, based on active compliance regulation of the CoM [34],
- an active foot tilting controller [35] that reacts to disturbances by tilting the feet to lift the CoM,
- a stepping maneuver [36],

to verify the simulation results due to the higher degree of stability introduced by the use of the balancing controllers.

In Fig. 3, the panels (a) to (i), show the performed simulations. C_1 represents the standard COMAN robot with all joints stiffly controlled in position. In C_2, the compliant stabilizer [34] is enabled. In C_3, the foot tilting controller [35] is enabled. In C_4, the stepping maneuver [36] is enabled. C_5 and C_6 represent configurations with half and double the foot length, respectively.

W_1 denotes the standard WALK-MAN robot with all joints stiffly controlled in position, while W_2 and W_3 represent configurations with half and double the foot length, respectively.

Table II presents the final benchmarked data regarding each robot. When comparing the COMAN and WALK-MAN directly, it can be seen that the WALK-MAN could withstand a much higher disturbance. W_1 can endure up to an absolute normalized angular momentum of 3.175. Compared to C_1 with 0.367, and 1.0 for a human, W_1 shows almost 8 times more absolute stability than C_1, which is reasonable considering its larger foot size and heavier mass. However, W_1's relative stability, 1.305, is smaller than C_1's 1.341 if normalized *w.r.t* their LIPM. These results emphasize the importance of having a proper bench to compare the hardware designs from the stability point of view regarding the robot dimensions. C_2 shows the robot's behavior when a compliant stabilizer

is enabled. The robot's stability decreased, both absolutely and relatively, due to the balancing capability being traded off for compliant behavior [34] introduced by the controller. C_3, which uses a foot tilting controller [35] on the other hand, generates higher stability due to its active effort to maintain balance. C_4, which inherits a stepping maneuver [36], has the highest stability of all COMAN subjects, thanks to the step completing counteracting the falling action. C_5 and C_6 also demonstrate intuitive results due to the decrease and increase in normalized angular momentum of both models respectively, with W_2 and W_3 commends this result.

IV. EXPERIMENTAL RESULTS ON THE THERAPEUTIC EXOSKELETON H3

The proposed benchmark was further tested on the H3 exoskeleton (Exo-H3), both in simulation and on real hardware. The Exo-H3 is a wearable lower limb exoskeleton that provides bilateral traction with six degrees of freedom, three in each leg, actuated by brushless direct current motors. These motors enable hip, knee, and ankle rotations in the sagittal plane. Each joint is equipped with position and force sensors, as well as two pressure sensors on each foot. Designed specifically for research purposes, the Exo-H3 permits the implementation of new algorithms and control strategies [37]. The hardware can be adapted to the user's anthropometric characteristics by adjusting its geometry. When wearing it, a person with complete or incomplete spinal cord injury affecting the lower extremities can walk using their legs with the aid of crutches or similar support elements and/or with the help of a health professional. The Exo-H3 weighs 15.384 kg, with a CoM height of $z_0 = 0.567$ m, and a foot sole size of 0.3 m. Given these quantities, we can obtain the time constant $T_c = \sqrt{z_0/g} = 0.24$ s, and $x_{cp}^{max} = 0.15$ m.

A. SETUP

To apply the proposed benchmark to the Exo-H3, the robot was positioned with the knees partially bent, at 10% of the leg length, and the CoM placed in the center of the support polygon in agreement with Fig. 2. As seen in Fig. 4 the robot was hung from a static structure and secured through a holding system to prevent damage during falling. The system, reported in [38], was designed as an Ambulatory User Support Gait Rehabilitation Robot under the Spanish National Project, *Nimble*. In addition, a force-sensing resistor (FSR) sensor was calibrated and placed at the back of the pelvis to measure the applied impulse with $l_{\text{imp}}^* = 0.787$ m. A frontal holder was used to prevent the pelvis from spreading keeping the desired position during the experiments. The force data were captured at 100 Hz and processed in Matlab. Subsequently, a series of separate experiments were conducted, in which the Exo-H3 either fell or did not. The robot was pushed manually applying an impulse force directly on the sensor. It is important to note that the experiments considered were those where the tilting performance was at its limit: soft or overly powerful impulses were discarded. Additionally, we only considered experiments in which the measured maximum force was

FIGURE 4: Experimental setup for the H3 exoskeleton.

greater than 30 N with an impulse duration $t_{\text{imp}} < 0.24$ s. This approach ensured the collection of sufficient statistical data to evaluate the Exo-H3's performance under the proposed benchmark. As shown in Fig. 5, the considered experiments are close to each other, providing an adequate perspective on the proposed data analysis, with a total of 149 recorded experiments.

To validate the initial impulse defined in Section II-A (see Fig. 1(a)), we extracted the mean linear momentum obtained from the experimental data using (3). Consequently, we selected the mean peak force value that caused the robot to fall, $F_{\text{imp}}^* = 37.6$ N, and the associated mean impact duration time $t_{\text{imp}} = 0.193$ s. Using the equivalent force at the CoM, computed with (19), $F_{\text{imp}} = 53.2$ N, we calculated the linear momentum $p_{\text{imp}} = 6.53$ Ns using (3). This value represents the mean linear momentum required to make the Exo-H3 fall when subjected to a pure sinusoidal impulse.

The linear momentum variation for the falling cases when using (3) is seen in Fig. 6. The abscissa indicates how the momentum was computed: either using a pure sinusoidal impulse (3) or using the integral over the recorded disturbance (1). Falling cases are shown in red, while non-falling cases are shown in blue. As seen in the first box plot, the momentum ranges from a minimum value of 4.1 Ns to 8.1 Ns. Comparing this with the non-falling cases, where the linear momentum was calculated using (3) (shown in Fig. 6), we see that the mean value is $p_{\text{imp}} = 6.14$ Ns, which is smaller than the 6.53 Ns obtained for the falling cases. However, there are instances where the linear momentum of a single experiment exceeds 6.53 Ns without causing the robot to fall. This occurs due to the interaction between the robot and the applied disturbance, requiring a larger linear momentum for faster disturbances, as will be analyzed later. When calculating the linear momentum over the recorded disturbance using (1), with a sampling time of 0.01 s, we can verify the consistency in the analysis validating the definition in Section II-A for applying the proposed benchmark.

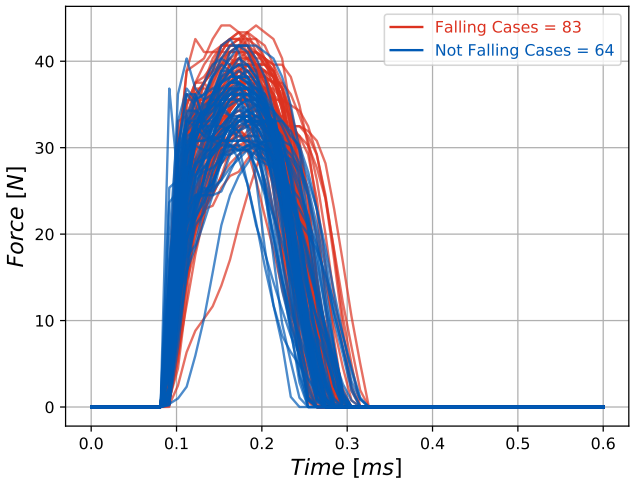

FIGURE 5: Applied forces during experiments. Record Experiments with $t_{\text{imp}} < T_c$ and $A_{\text{imp}} > 30$ N on the H3 exoskeleton.

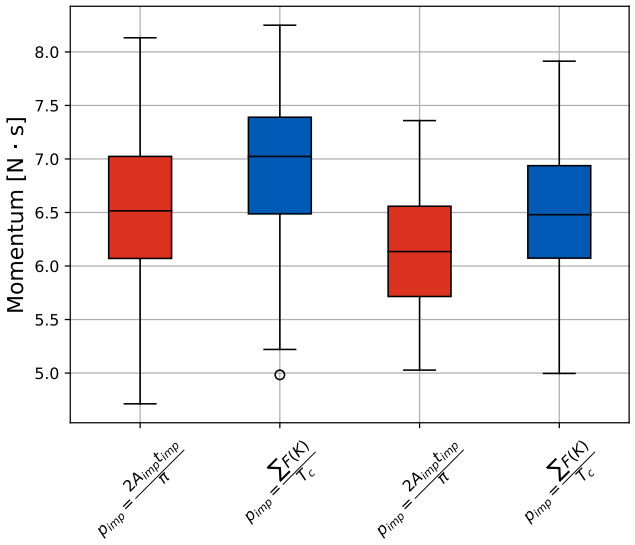

FIGURE 6: Applied momentum calculated using (3) and (1) to the H3 exoskeleton for Falling Cases (in red) and Not Falling Cases (in blue). Case $H3_1$.

B. RESULTS

Table III reports the number of Falling Cases for Exo-H3 for the recorded force applied on the real hardware, and corresponding median linear momentum $\bar{p}_{imp}$ before falling, calculated as in (1). $H3_1$ refers to the real Exo-H3. $H3_2$ to $H3_5$ correspond to simulations using various lengths of the foot soles: 0.227 m, 0.23 m, 0.235 m, and 0.24 m, respectively. In $H3_6$, we compute the foot size such that the linear momentum corresponds to that of $H3_1$, but with a shorter impact duration of $t_{\text{imp}} = 0.12$ s. In $H3_7$ an impulse with $t_{imp} = 0.12$ s and a p_{imp} equal to the one on $H3_2$ was used, later, the foot length was continuously increased till reaching the tilting point which is 0.235 m. Finally, $H3_8$ corresponds to the simulation of the H3 exoskeleton when using a rigid sole of 0.3 m as in $H3_1$.

We evaluated the performance of the simulated robots using a model built in SimMechanics® [23]. In this model, the foot sole is rigid, which leads to interaction forces with the ground that differ from those of the real robot, resulting in better balance performance than the actual hardware. Consequently, it is necessary to simulate the robot while adjusting the sole size to more accurately reflect the balance behavior observed in the experimental scenario. For this purpose, we used a simulated impulse, as shown in Fig. 1(a), with mean values obtained from the experimental data, i.e., an impulse duration $t_{\text{imp}} = 0.197 \approx 0.2$ s and an applied force at the hip $F^*_{\text{imp}} = 37.6$ N. With the applied impulse, the foot length that mimics the real robot's behavior during falling was found to be 0.227 m. This results in a total CoM travel distance of 0.077 m, in contrast to the 0.15 m travel distance of the real robot when the CoM is in the midpoint of the original feet before impact. This implies that a non-rigid sole can be modeled with a shorter rigid sole. From a different perspective, the proposed benchmark can be enhanced in the real robot by using more rigid sole materials.

In Fig. 7, we evaluate the linear momentum generated by the applied force data obtained in the experiments. These data were applied to the simulated Exo-H3 using different sole sizes, considering only those cases where the simulated robot fell. These simulations illustrate how modifications to the foot sole, or equivalently the sole material, affect the overall robot's performance. The linear momenta were calculated by integrating the recorded disturbance $F(k)$ with a sampling time of 0.01 s.

Comparing the performance of the simulated robot with a foot sole of 0.227 m to the original case, as shown in Table III, it is notable that the robot falls in ten additional experimental trials. However, there is less dispersion in the corresponding linear momenta, leading to a slightly higher mean value: 7 Ns for the real robot and 7.13 Ns for this case. As the sole size increases, the mean linear momentum also increases, as expected, and the number of falling cases decreases. With a sole size of 0.24 m, no experimental data caused the robot to fall in simulation. When applying a sinusoidal disturbance with $t_{\text{imp}} = 0.2$ s and increasing the applied force until reaching the stability limit, we obtained a linear momentum of $p_{\text{imp}} = 7.81$ Ns, which is smaller than the linear momentum of some of the existing experimental data. This occurs because a shorter impulse requires larger forces and, consequently, a larger overall linear momentum to affect the robot equivalently. This can be seen in the following two cases. The first case examines the required foot size to achieve a linear momentum of $p_{\text{imp}} = 6.637$ Ns, corresponding to the angular momentum for $H3_2$ in Table II, but with an impulse duration of $t_{\text{imp}} = 0.12$ s instead of the original 0.2 s. The second case investigates the required force on the hip and the linear momentum p_{imp} necessary to cause the robot to fall with a sole size of 0.227 m (the same as in $H3_2$ in Table II), but

TABLE III: Number of Falling Cases for real Exo-H3. $\bar{p}_{imp}$ represents the median linear momentum.

Case	Number of Falling Cases	$\bar{p}_{imp}$ (Ns)
$H3_1$	84	7.02
$H3_2$	94	7.13
$H3_3$	59	7.29
$H3_4$	25	7.55
$H3_5$	0	7.81

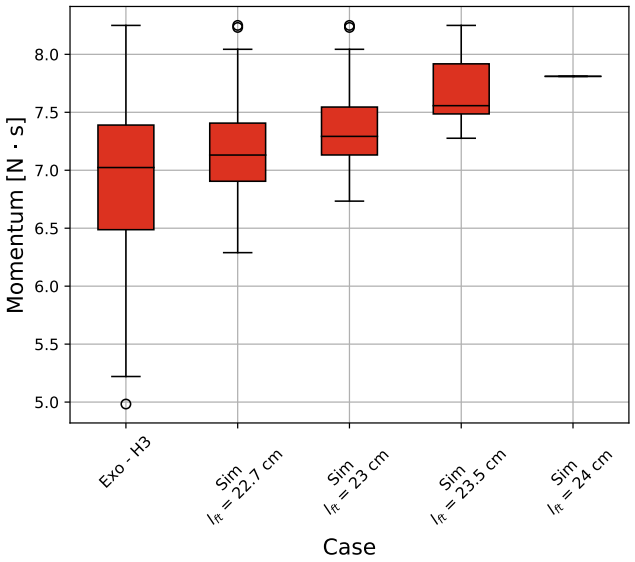

FIGURE 7: Falling Cases for real the robot and different sole sizes in simulation. H3 cases from $H3_1$ to $H3_5$.

using an impulse duration of $t_{\text{imp}} = 0.12$ s, corresponding to $(T_c/2)$ as in (18).

The resulting scenarios are reflected in Table II for the cases named $H3_6$ and $H3_7$, respectively. For $H3_6$ and $H3_2$, the $L_{\text{imp}} = 3.76$ Nms; however, the travel distance in $H3_6$ is 0.085 m, while in $H3_2$ it is 0.15 m. This indicates that a faster impulse requires a larger sole to be absorbed by the simulated Exo-H3. On the other hand, when comparing $H3_7$ and $H3_2$, the travel distance in both cases is 0.077 m. However, the linear momentum p_{imp} for $H3_7$ is $p_{\text{imp}} = 5.9$ Ns, which is smaller than the linear momentum in $H3_2$ of $p_{\text{imp}} = 6.6$ Ns obtained from the data. These cases, $H3_6$ and $H3_7$, imply that a faster impulse with the same amplitude introduces greater variations in the linear momentum of the hardware, which must be considered when applying the benchmark.

As shown in Table II, the experiments indicate that the Exo-H3 has an angular momentum benchmark of $\hat{L}^H_{imp} = 0.15$ relative to a human. However, an important result from the simulations reveals that the mechanical structure has the

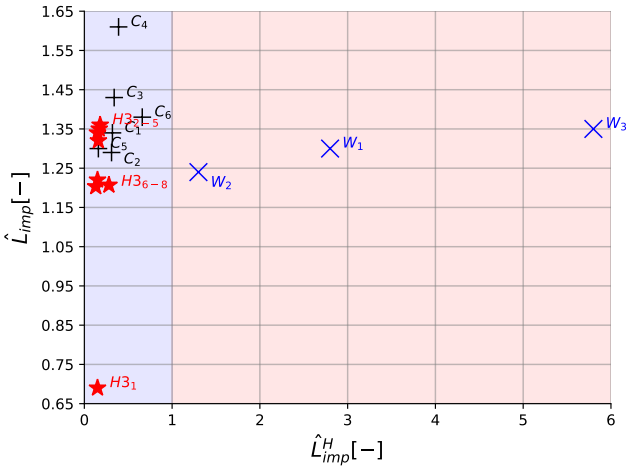

FIGURE 8: Benchmarked robot maximum standing stability by angular momentum ($\hat{L}_{\text{imp}}$ and $\hat{L}^H_{\text{imp}}$ in Table II).

potential to increase this benchmark to $\hat{L}^H_{imp} = 0.28$ by modifying the rigidity of the sole, which in the simulations corresponds to having a full-size sole. From this perspective, the proposed benchmark might help adjust the level of static balancing capabilities of the hardware.

This can also be used therapeutically by modifying the comfort level in the standing position of a patient according to their remaining abilities. By adjusting the inner exoskeleton's capability, rehabilitation therapy can provide the patient with either more or less stable hardware, promoting active balance training. Another interesting result from the present benchmark is that it allows us to determine the maximum external stimuli that a patient might experience while wearing the robot to maintain static stability. To achieve this, set-up experiments with the patient wearing the exoskeleton are required, but this case is not considered in the present work.

V. DISCUSSION

A graphical comparison of the normalized angular momentum for the different robots is presented in Fig. 8. The horizontal axis shows the robots' balancing capabilities compared to an average human model ($\hat{L}^H_{\text{imp}}$), while the vertical axis represents $\hat{L}^H_{\text{imp}}$ normalized by their respective LIPM.

The figure reveals that the WALK-MAN exhibits superior balancing capabilities compared to the average human model but shows relatively lower performance compared to other robots. In contrast, the COMAN demonstrates the opposite trend. Additionally, the Exo-H3 shows improved relative stability, although its performance relative to the human model does not increase significantly.

It is essential to further investigate the benchmark for the Exo-H3 when used by a human and to evaluate its potential to offer additional balance assistance to a hypothetical patient. Finally, in comparison to humanoid robots, the Exo-H3 is less stable. However, it is designed to be worn rather than used as an independent walker as a humanoid. Additionally, the

emphasis on keeping the equipment as lightweight as possible affects its balance performance.

Despite the flexibility and ease of application of the presented benchmark across different hardware, it is important to note its susceptibility to different disturbances characterization, as previously discussed. This sensitivity necessitates extensive experimentation to ensure that similar disturbances are obtained when using experimental data. Furthermore, normalizing using human quantities may require new parameterization depending on the application, particularly when using wearable systems, where benchmarking must consider the individual wearing the system. While this expands the applicability of the proposed method, it raises questions about how to define a standard human parametrization that stands for different cases.

In contrast, the LIMP provides a straightforward and effective comparison tool for evaluating the benefits of specific hardware designs. However, this model is constrained by fabrication limitations. As demonstrated in this study, the COMAN design appears more stable than the WALKMAN design. Nevertheless, constructing a COMAN of such dimensions may result in unanticipated behaviors that diverge from benchmark predictions. Consequently, this benchmark may be best suited for comparing hardware with similar characteristics.

From the perspective of wearable systems, the present benchmark can be used to test the effect that the wearable system has over the user in different areas, testing the balance capabilities when wearing or not the hardware. In that sense, this benchmark might be used to study the potential hazards when wearing the system in therapeutic or industrial environments. However, it is required to consider the additional stochastic variability that involving humans introduces into the benchmark, particularly in patients with limited mobility. Moreover, in therapeutic scenarios, ensuring the safety of patients during fall tests imposes additional constraints that could limit the applicability of the benchmark.

VI. CONCLUSION AND FUTURE WORKS

In this paper, a benchmarking metric for the standing stabilization of bipedal robots has been developed. The method provides a quantitative approach to compare the maximum standing stability of bipedal robots of any size using both relative and absolute measures. The proposed method tests not only the mechanical stability but also the effectiveness of balancing controllers.

Relative benchmarking offers a rational approach to comparing performance and balancing characteristics across different robots. It can also serve as a design tool and supplementary analysis for comparable bipeds or specific hardware. This allows for the comparison of different structural configurations of the same robot, providing insights into its potential capabilities before or after manufacturing. Additionally, the benchmark is intuitive and useful for analyzing various balancing algorithms, enabling designers to easily measure their success.

The proposed benchmark assesses stability by inducing a disturbance in the sagittal direction but can be applied to any standing sensorimotor task in any posture. For instance, a robot on an inclined plane with a lateral disturbance would require the same parameters plus a new derivation of α incorporating the plane's angle. The scheme benchmarks not only standing stability but also additional control strategies such as balancing or stepping. Performance can be compared to the LIPM as a cross-validation indicator or with human normalization, crucial for future work on wearable systems.

The proposed benchmark was tested in simulation on both the humanoid and exoskeleton, as well as on the real H3 exoskeleton. The results highlight the significant impact of sole design on the exoskeleton's performance, suggesting that optimizing the sole design can enhance the level of assistance during recovery if needed.

Future work will include additional physical tests of exoskeletons, particularly therapeutic lower-limb exoskeletons for rehabilitation, involving both healthy subjects and patients. These tests will evaluate the proposed benchmark as a therapeutic indicator and correlate the intrinsic balance capability of the hardware with therapeutic success. Additionally, the benchmark metrics will be extended to quantify the effects of pushing the robot from different directions and its performance on various terrains. Finally, extensions of this work will develop benchmarks for dynamic stability in robots and wearable systems.

References

[1] D. Torricelli *et al.*, "Benchmarking bipedal locomotion: A unified scheme for humanoids, wearable robots, and humans," *IEEE Robotics & Automation Magazine*, vol. 22, no. 3, pp. 103–115, 2015.

[2] D. Torricelli *et al.*, "Benchmarking human-like posture and locomotion of humanoid robots: A preliminary scheme," in *Conference on Biomimetic and Biohybrid Systems*, 2014, pp. 320–331.

[3] D. Torricelli *et al.*, "Human-like compliant locomotion: State of the art of robotic implementations," *Bioinspiration & Biomimetics*, vol. 11, no. 5, p. 051 002, 2016.

[4] K.-L. Ho Hoang, S. I. Wolf, and K. Mombaur, "Benchmarking stability of bipedal locomotion based on individual full body dynamics and foot placement strategies–application to impaired and unimpaired walking," *Frontiers in Robotics and AI*, vol. 5, p. 117, 2018.

[5] A. Hof, M. Gazendam, and W. Sinke, "The condition for dynamic stability," *Journal of Biomechanics*, vol. 38, no. 1, pp. 1–8, 2005.

[6] J. A. Castano, J. Humphreys, E. Mingo Hoffman, N. Fernández Talavera, M. C. Rodriguez Sanchez, and C. Zhou, "Benchmarking dynamic balancing controllers for humanoid robots," *Robotics*, vol. 11, no. 5, 2022.

[7] M. F. Hamza, R. A. R. Ghazilla, B. B. Muhammad, and H. J. Yap, *Balance and stability issues in lower extremity exoskeletons: A systematic review*, Oct. 2020.

[8] T. H. Hsu, C. L. Tsai, J. Y. Chi, C. Y. Hsu, and Y. N. Lin, "Effect of wearable exoskeleton on post-stroke gait: A systematic review and meta-analysis," *Annals of Physical and Rehabilitation Medicine*, vol. 66, 1 Feb. 2023.

[9] A. L. Hof, "Scaling gait data to body size," *Gait & posture*, vol. 3, no. 4, pp. 222–223, 1996.

[10] E. A. Fleishman, M. K. Quaintance, and L. A. Broedling, *Taxonomies of human performance: The description of human tasks.* Academic Press, 1984.

[11] S. Behnke, "Robot competitions-ideal benchmarks for robotics research," in *IEEE IROS 2006 - Workshop on Benchmarks in Robotics Research*, 2006.

[12] O. Stasse *et al.*, "Benchmarking the hrp-2 humanoid robot during locomotion," *Frontiers in Robotics and AI*, vol. 5, p. 122, 2018.

[13] S. Kajita, F. Kanehiro, K. Kaneko, *et al.*, "The 3D linear inverted pendulum mode: A simple modeling for a biped walking pattern generation," in *International Conference on Intelligent Robots and Systems*, vol. 1, 2001, pp. 239–246.

[14] N. Motoi, T. Suzuki, and K. Ohnishi, "A bipedal locomotion planning based on virtual linear inverted pendulum mode," *IEEE Transactions on Industrial Electronics*, vol. 56, pp. 54–61, 2009.

[15] F. Parietti and H. Geyer, "Reactive balance control in walking based on a bipedal linear inverted pendulum model," in *IEEE Conference on Robotics and Automation*, 2011, pp. 5442–5447.

[16] H. Dau, C.-M. Chew, and A.-N. Poo, "Proposal of augmented linear inverted pendulum model for bipedal gait planning," in *IEEE Conference on Intelligent Robots and Systems*, 2010, pp. 172–177.

[17] J. Pratt, J. Carff, S. Drakunov, and A. Goswami, "Capture point: A step toward humanoid push recovery," in *IEEE-RAS International Conference on Humanoid Robots*, 2006, pp. 200–207.

[18] Y. Kang, Z. Tian, and M. Zhao, "The ICP-based controllability criterion and its application to bipedal walking control," in *IEEE International Conference on Robotics and Biomimetics*, 2017, pp. 2425–2432.

[19] S. Gonzalez, P. Stegall, S. M. Cain, H. C. Siu, and L. Stirling, "Assessment of a powered ankle exoskeleton on human stability and balance," *Applied Ergonomics*, vol. 103, Sep. 2022.

[20] S. Dooley, S. Kim, M. A. Nussbaum, and M. L. Madigan, "A passive leg-support exoskeleton adversely affects reactive balance after simulated slips and trips on a treadmill," *Journal of Biomechanics*, vol. 151, Apr. 2023.

[21] J. H. Park, S. Kim, M. A. Nussbaum, and D. Srinivasan, "Effects of two passive back-support exoskeletons on postural balance during quiet stance and functional limits of stability," *Journal of Electromyography and Kinesiology*, vol. 57, Apr. 2021.

[22] J. H. Park, Y. Lee, M. L. Madigan, S. Kim, M. A. Nussbaum, and D. Srinivasan, "Wearing a back-support exoskeleton impairs single-step balance recovery performance following a forward loss of balance – an exploratory study," *Journal of Biomechanics*, vol. 144, Nov. 2022.

[23] l. m. Technaid, *User manual exo-h3*, Technaid S.L., Madrid, Spain, Aug. 2023.

[24] A. Okunola, A. Akanmu, and H. Jebelli, "Fall risk assessment of active back-support exoskeleton-use for construction work using foot plantar pressure distribution," *Advanced Engineering Informatics*, vol. 62, Oct. 2024.

[25] S. Fox, O. Aranko, J. Heilala, and P. Vahala, *Exoskeletons: Comprehensive, comparative and critical analyses of their potential to improve manufacturing performance*, Nov. 2020.

[26] G. Andersson, J. Hagman, R. Talianzadeh, A. Svedberg, and H. C. Larsen, "Effect of cognitive load on postural control," *Brain Research Bulletin*, vol. 58, no. 1, pp. 135–139, 2002.

[27] S. D. Bock *et al.*, *Benchmarking occupational exoskeletons: An evidence mapping systematic review*, Jan. 2022.

[28] C. Bayón *et al.*, "Development and evaluation of benchbalance: A system for benchmarking balance capabilities of wearable robots and their users," *Sensors*, vol. 22, 1 Jan. 2022.

[29] S. C. Walpole, D. Prieto-Merino, P. Edwards, J. Cleland, G. Stevens, and I. Roberts, "The weight of nations: An estimation of adult human biomass," *BMC Public Health*, vol. 12, 2012.

[30] A. M. Fredriks, S. van Buuren, W. J. M. van Heel, R. H. M. Dijkman-Neerincx, S. P. Verloove-Vanhorick, and J. M. Wit, "Nationwide age references for sitting height, leg length, and sitting height/height ratio, and their diagnostic value for disproportionate growth disorders," *Archives of Disease in Childhood*, vol. 90, no. 8, pp. 807–812, 2005.

[31] M. Diehl and K. Mombaur, *Fast Motions in Biomechanics and Robotics: Optimization and Feedback Control*. Jan. 2006, vol. 340.

[32] N. G. Tsagarakis, S. Morfey, G. M. Cerda, Z. Li, and D. G. Caldwell, "Compliant humanoid COMAN: Optimal joint stiffness tuning for modal frequency control," in *IEEE International Conference on Robotics and Automation*, 2013, pp. 673–678.

[33] N. G. Tsagarakis *et al.*, "Walk-man: A high-performance humanoid platform for realistic environments," *Journal of Field Robotics*, vol. 34, no. 7, pp. 1225–1259, 2017.

[34] C. Zhou, Z. Li, X. Wang, N. Tsagarakis, and D. Caldwell, "Stabilization of Bipedal Walking Based on Compliance Control," *Autonomous Robots*, vol. 40, pp. 1041–1057, 2016.

[35] Z. Li, C. Zhou, Q. Zhu, and R. Xiong, "Humanoid Balance Recovery with Actively Controlled Underactuation," *IEEE Transactions on Robotics*, vol. 33, no. 2, pp. 298–312, 2017.
[36] R. Wang, S. Hudson, Y. Li, H. Wu, and C. Zhou, "Normalized neural network for energy efficient bipedal walking using nonlinear inverted pendulum model," in *IEEE International Conference on Robotics and Biomimetics*, Dali, China, Dec. 2019, pp. 1399–1405.
[37] J. Ramos-Rojas, J. S. Lora-Millán, J. A. Castano, J. Carballeira, P. R. Fernández, and S. Borromeo, "Diseño conceptual de un robot de rehabilitación de la marcha pseudoestacionario," *Revista Iberoamericana de Automática e Informática industrial*, Jun. 2024.
[38] J. Ramos-Rojas *et al.*, "Design and validation of an ambulatory user support gait rehabilitation robot: Nimble," *Actuators*, vol. 13, no. 9, 2024.

JUAN A. CASTANO received the B.S. and M.S. degrees in electronic engineering from the Pontifical Xavierian University, Bogotá Colombia, in 2011 and the Ph.D. degree in Robotics, Cognition and Interaction Technologies, in 2016 at the Genoa University, Genoa, Italy. Nowadays is an assistant professor at the King Juan Carlos University, Madrid, Spain. His research interests include Control Techniques, System Identification based on data drive algorithms, Humanoid locomotion, and Neurorehabilitation strategies with exoskeletons.

EUGENIO MANUEL ESPUELA is currently pursuing a Master's degree in Industrial Engineering at the Universidad Rey Juan Carlos, where he specializes in electronics, robotics, and automation. His research focuses on rehabilitation exoskeletons, aiming to enhance their efficiency and accessibility for patients. Before starting his Master's program, Eugenio graduated with a degree in Industrial Technologies Engineering from the Universidad Rey Juan Carlos. He has two years of experience collaborating with the BeST group on the Nimble project, where he contributed to the development and testing of advanced robotic control systems for rehabilitation.

JAIME RAMOS ROJAS received the B.S. and M.S. degrees in Biomedical Engineering from the Polytechnic University of Madrid and Politecnico di Milano, respectively, in 2018. Currently, he is a PhD Student at Rey Juan Carlos University in Madrid, Spain, at the Department of Applied Mathematics, Science and Material Engineering, and Electronics Technologies. His research focuses on biomechanics of human movement & robotic assistance devices for rehabilitation.

ENRICO MINGO HOFFMAN is a permanent researcher at Inria Centre, Université de Lorraine. He received his Ph.D. degree in Robotics in 2016 from the University of Genoa and Istituto Italiano di Tecnologia. His research focuses on whole-body loco-manipulation planning and control of multi-limbed systems, optimization, and optimal control.

CHENGXU ZHOU is an Associate Professor in Robotics and AI at the Department of Computer Science, University College London. He received his Ph.D. degree in Robotics in 2016 from the Italian Institute of Technology. His research focuses on developing intelligent motion generation for legged robots, with a particular emphasis on dynamic motion planning and whole-body control of articulated robots using optimization & machine learning technologies.